

Electronic Supplementary Information

Template Assisted Preparation of High Surface Area Macroporous Supports with Uniform and Tunable Nanocrystal Loadings

Michael T.Y. Paul, Brenden B. Yee, Xin Zhang, Eiji H. Alford,

Brandy K. Pilapil, and Byron D. Gates*

Department of Chemistry, Simon Fraser University

8888 University Drive, Burnaby, B.C. V5A 1S6, Canada

*bagtes@sfu.ca

Acknowledgements

Financial support for this work was provided by the Natural Sciences and Engineering Research Council (NSERC) of Canada Discovery Program (Grant No. 1077758), CMC Microsystems (MNT Grant No. 2152), Canada Research Chairs Program (B.D. Gates; Grant No. 950-215846), and the Engineered Nickel Catalysts for Electrochemical Clean Energy project administered from Queen's University and supported in part by Grant No. RGPNM 477963-2015 from the NSERC of Canada Discovery Frontiers Program. This work made use of 4D LABS (www.4dlabs.ca) and the Centre for Soft Materials shared facilities supported by the Canada Foundation for Innovation (CFI), British Columbia Knowledge Development Fund (BCKDF), Western Economic Diversification Canada, and Simon Fraser University. We would like to thank Mr. Austin (Woo hyuk) Lee for performing physical vapor deposition of Au and TiO₂ thin films, and Dr. John-Christopher Boyer for providing the NaYF₄ nanoparticles for use in this study.

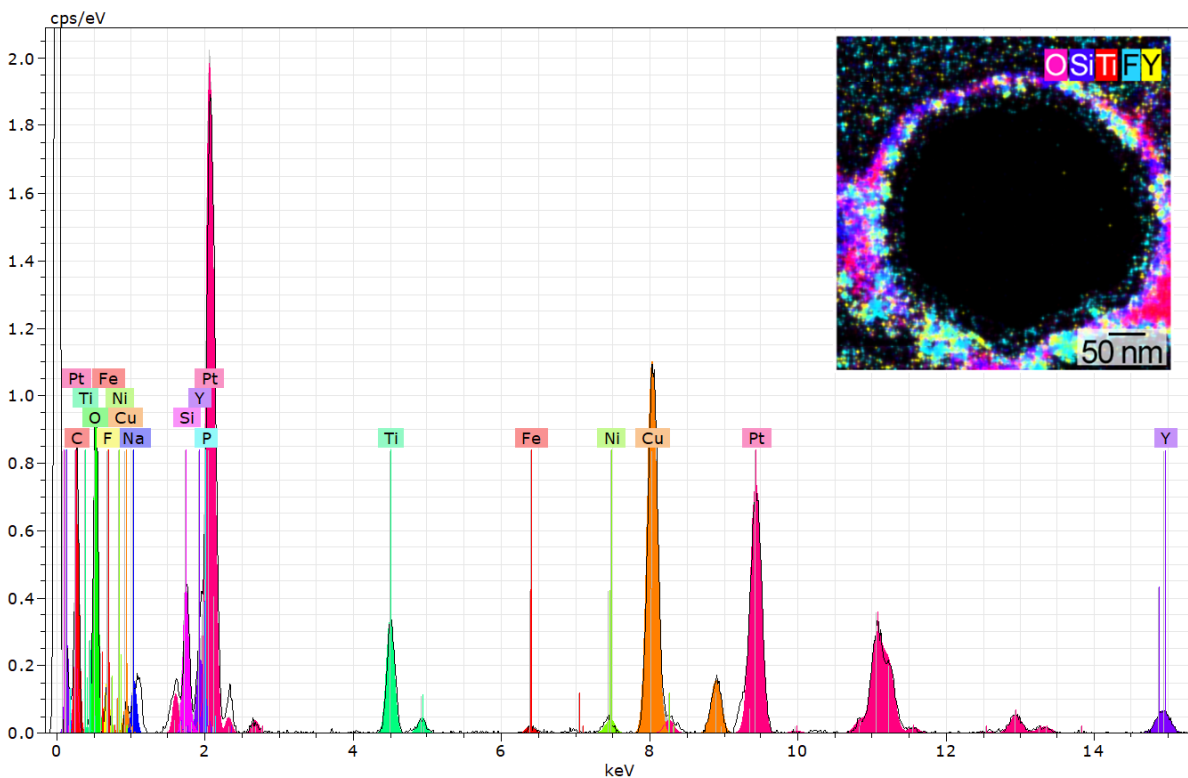


Figure S1. Deconvoluted spectrum obtained by transmission electron microscopy (TEM) techniques using energy dispersive X-ray spectroscopy (EDS) of upconverting nanocrystal (UCNC) coated, macroporous metal oxide support. Some additional elements including Fe, F, and Ni could be a result of environmental contaminations from the machine hardwares and other chemicals present in the laboratory. The Cu signal is generated from the TEM grid. The inset image depicts the corresponding EDS map of the respective sample.

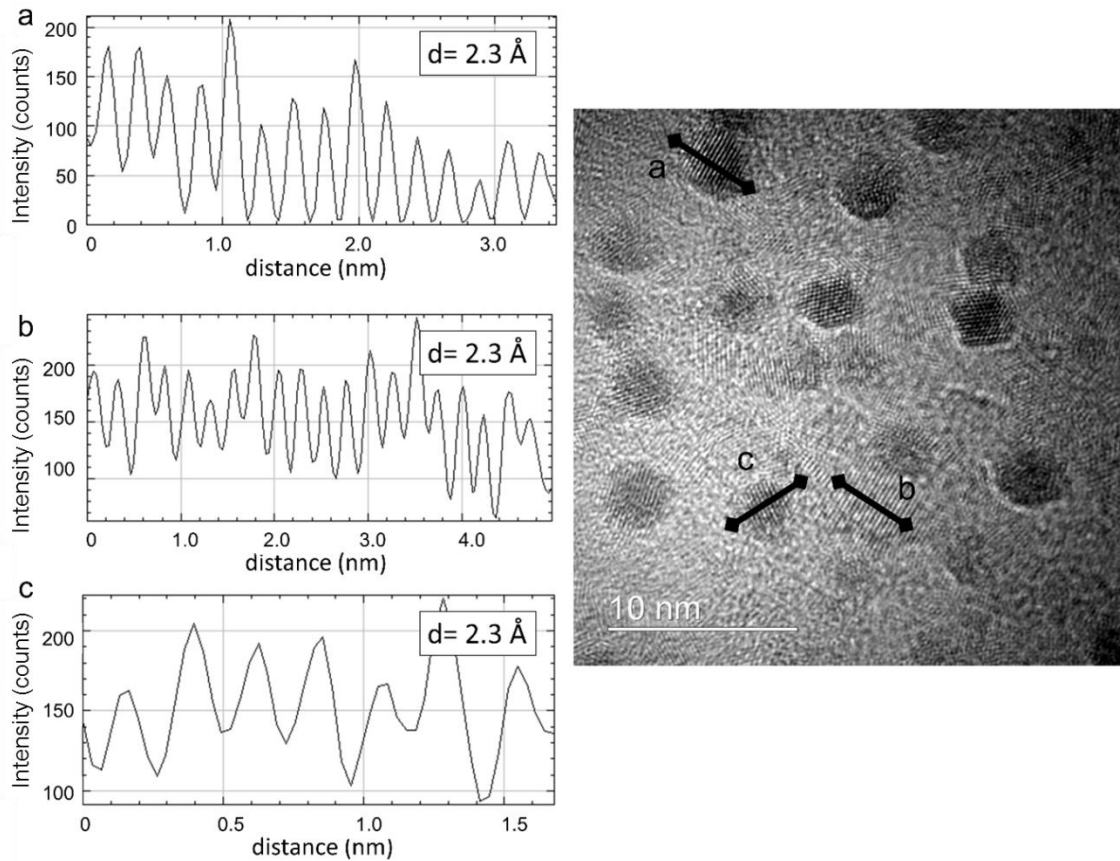


Figure S2. High resolution transmission electron microscopy (HRTEM) images of Pt nanocrystals (NPs) depicting their lattice fringes. The lines a, b, and c correspond to the intensity profiles in the associated plots. These results indicated the lattice fringes had an average spacing of 2.3 \AA , which matches d-spacing for the Pt (111) facets.

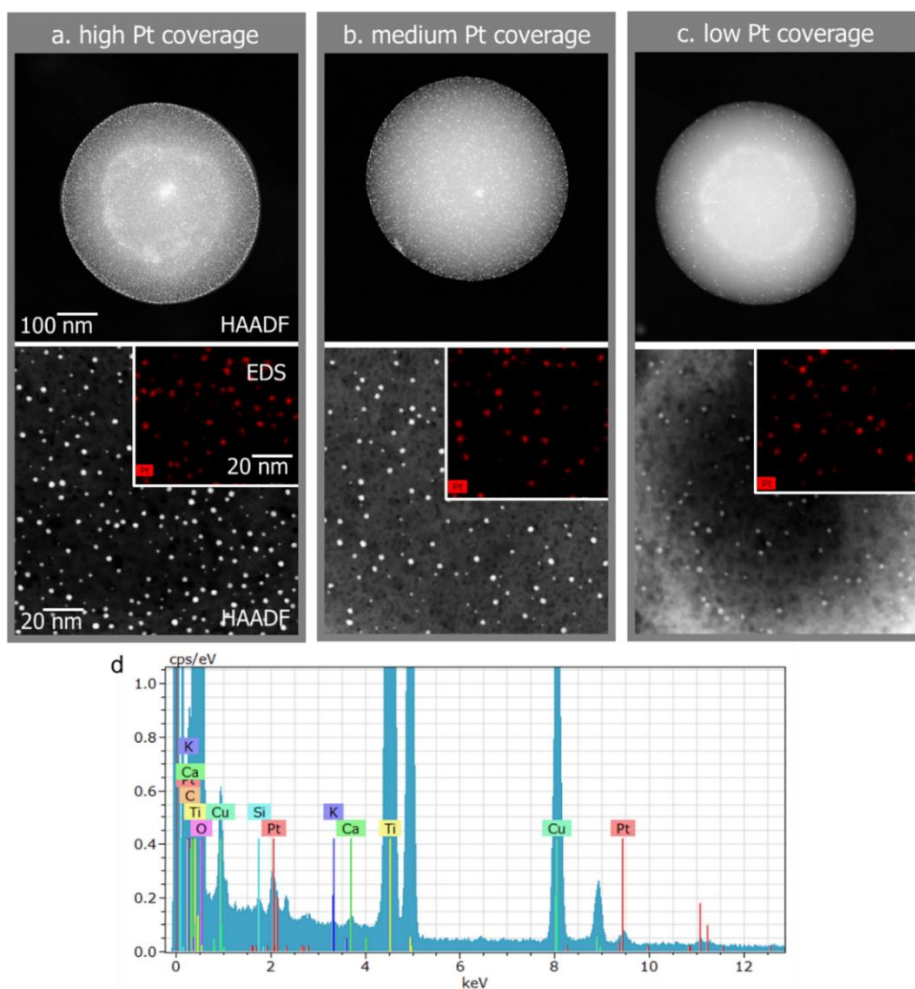


Figure S3. Images of polystyrene (PS) spheres with high, medium, and low coverages of Pt NPs and their corresponding transfer onto a porous TiO₂ support are shown in columns a, b, and c, respectively. The top image for each column is a representative high angle annular dark field (HAADF) STEM image of the loadings of Pt NPs on the spherical templates. The bottom images consist of representative HAADF STEM images of Pt NPs immobilized on TiO₂ supports, and the inset images are the EDS elemental maps of the Pt NPs on the TiO₂ support. The scale bars in column a apply to the corresponding images in columns b and c. A corresponding EDS spectrum for these samples is presented in (d), note residual contaminations from NP synthesis could be present including K and Ca; the Cu arises from the TEM grid material.

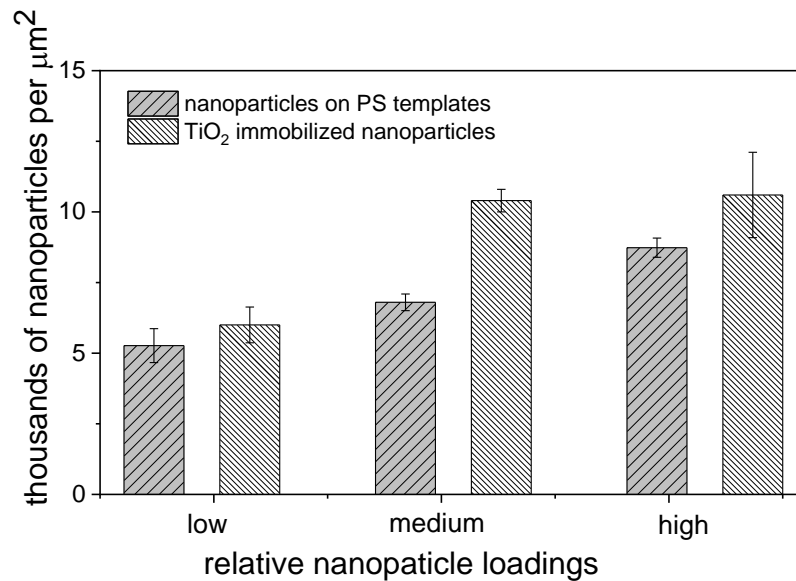


Figure S4. Statistical analyses of the number of Pt NPs loaded onto the spherical PS templates, and the number of Pt NPs immobilized on the porous TiO₂ supports after further processing of these templates. At least ~5000 NPs were manually counted for each of the samples, the error bars account for \pm one standard deviation from the averaged measurements.

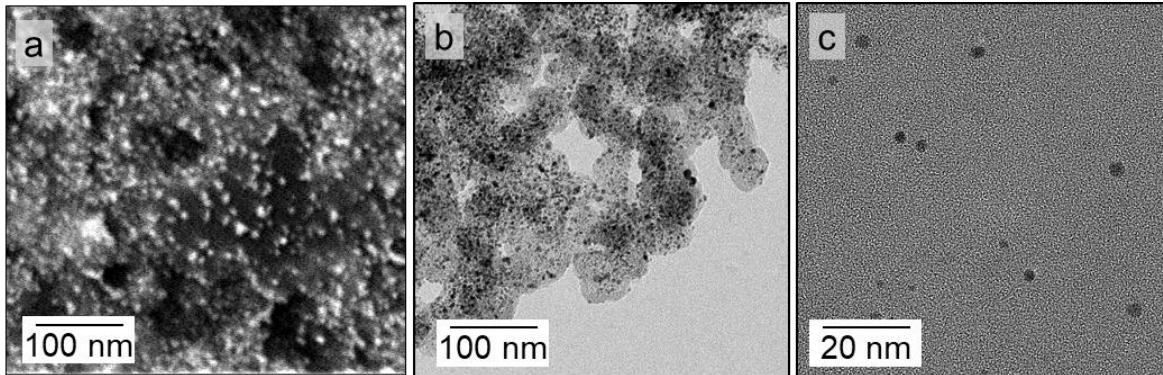


Figure S5. Electron microscopy images of a mixture of Pt and carbon nanocrystals (Tanaka Holdings Corp., Ltd.; TEC10E50E): (a) a scanning electron microscopy (SEM) image obtained using a concentric backscatter detector to highlight the locations of the Pt NPs within this mixture; (b) a similar magnification TEM image of the sample in (a); and (c) a relatively high magnification TEM image of the sample depicting the spacing between the Pt nanocatalysts.

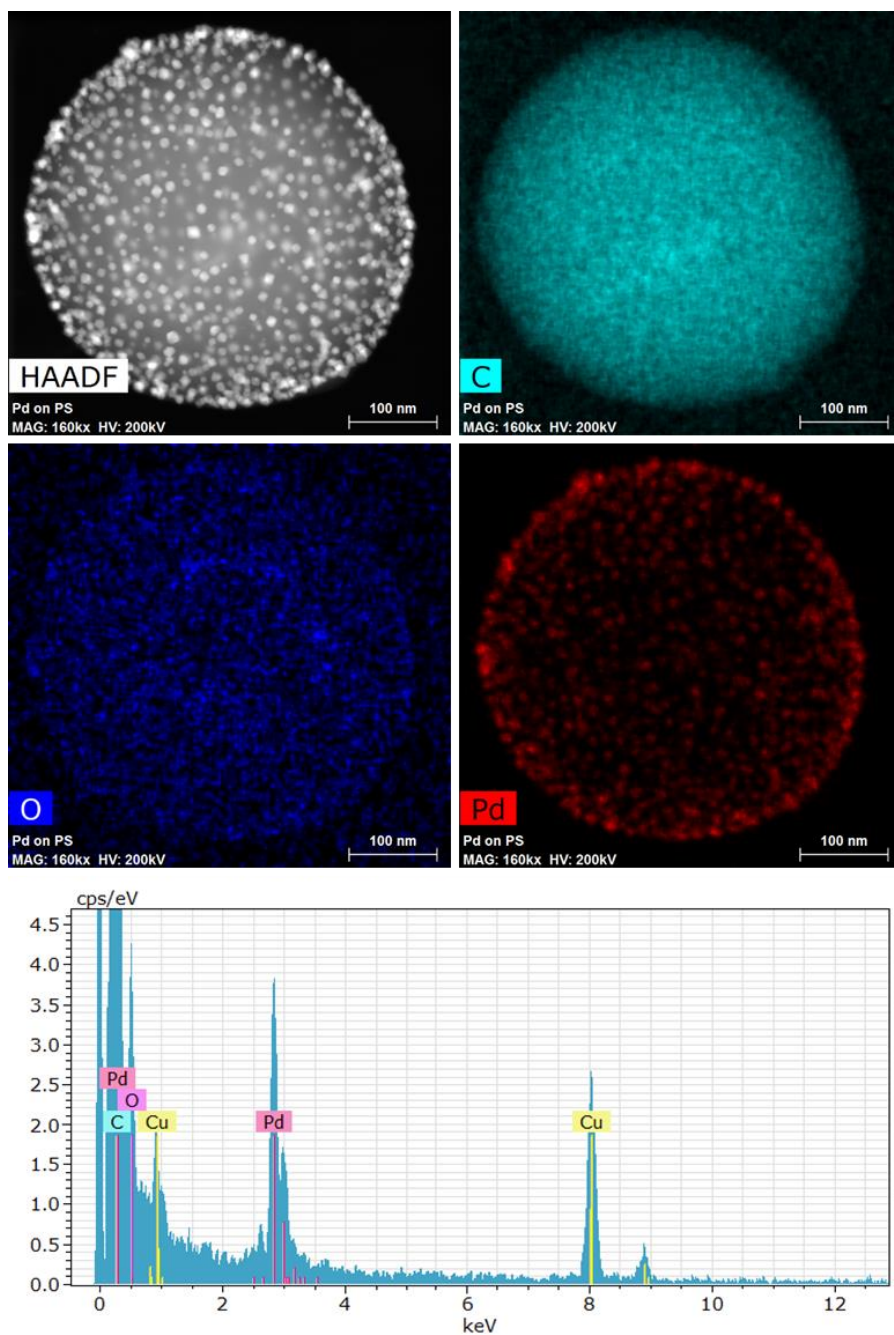


Figure S6. A series of TEM images including a HAADF analysis and EDS elemental maps of Pd NPs (13 ± 2 nm \varnothing) coated onto spherical PS templates (~ 400 -nm \varnothing), which were used for the preparation of hexagonally close-packed arrays of dimpled Ni that supported the Pd NPs as a structured electrocatalyst. The corresponding EDS spectrum for this sample is presented at the bottom of the EDS maps.

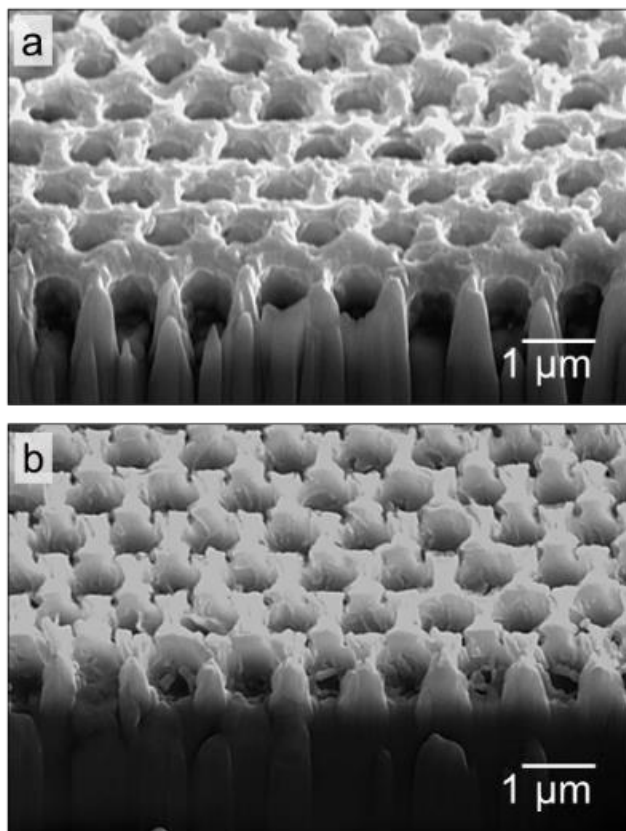


Figure S7. Cross-sectional SEM images of dimpled features in Ni after template removal: (a) Ni electrodeposited to cover approximately $2/3$ of the height of the polymer templates; and (b) Ni electrodeposited to cover approximately $1/2$ of the height of the polymer templates.

Electrochemical Oxidation of Methanol Catalyzed with Ni Supported Pd Nanocrystals

A series of electrochemical experiments were performed to investigate the utility of the ordered arrays of dimpled Ni that supported Pd nanocrystals as a high surface area electrode. The measurements were performed with a Biologic Science Instruments SP-150 potentiostat. Electrochemical data was collected using the EC-Lab data analysis software (V10.18). The customized electrodes were each incorporated as the working electrode into a typical three electrode set-up using a custom glass electrochemistry cell with a single junction, 10-mm diameter, Ag/AgCl reference electrode, and a Pt wire (0.6-mm diameter; 99.98%; Alfa Aesar) counter electrode. The electrochemical solution, consisting of 10 mM of methanol (99.9%, Fisher Chemical, United States) and 0.5 mM of KOH (85%, Macron Fine Chemicals, United States), were purged with N₂ gas (99.98%, Praxair, Canada) for at least 30 min prior to the commencement of the experiments. A positive N₂ gas pressure was maintained in the head space of the electrochemical cell throughout the experiments. Cyclic voltammetry (CV) measurements of methanol oxidation were performed at a scan rate of 20 mV/s, with a sweep range from -0.8 to 0.3 V, at 21 ± 0.2 °C, and without perturbation of the solution. The potential applied to the sample was repeatedly scanned until reaching stabilization of the peak current for methanol oxidation (<10 μA deviation in current). The stabilized CV scan profiles were normalized against the Pd electrochemically active surface area (ECSA). This normalization enabled a comparison of the Pd mass activity for the Pd NPs supported on dimpled Ni to the planar (100 nm of Pd on 10 nm of Cr) Pd electrodes created by electron beam deposition (93%, Pd pellets, Kurt J. Lesker, PVD75, United States). The Pd ECSAs were estimated from the integrated area for the Pd oxide reduction peak in the CV profiles, assuming the charge associated with the reduction of the oxygen monolayer is 420 μC/cm².¹⁻²

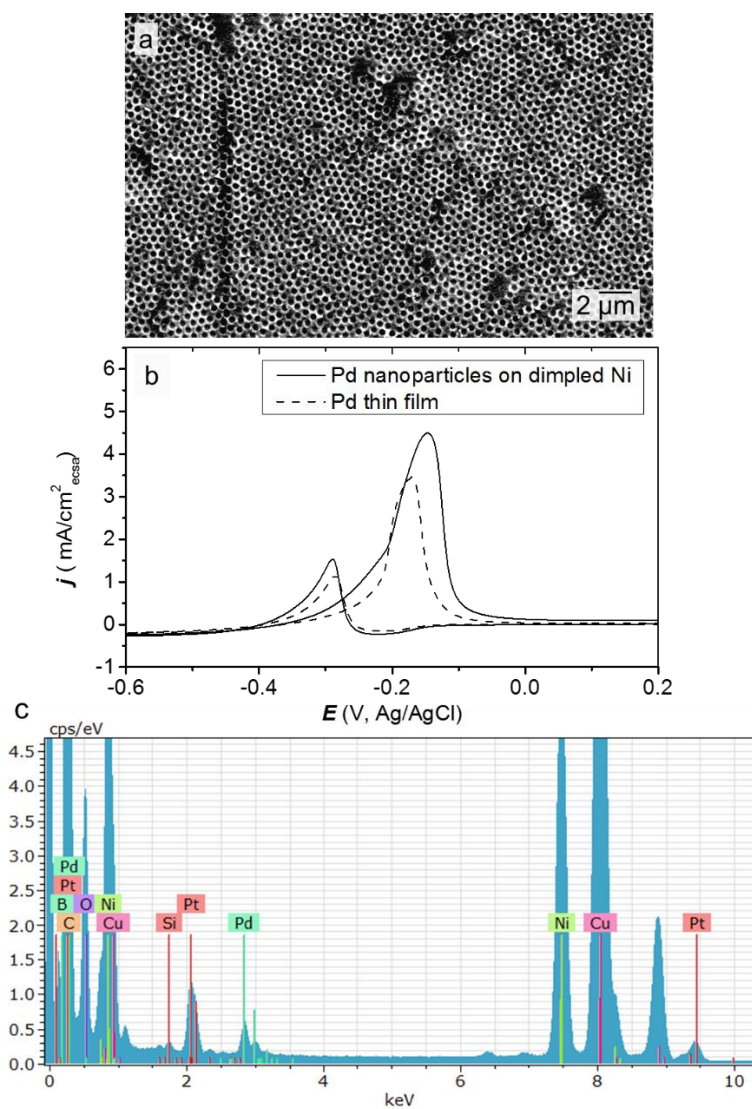


Figure S8. (a) The SEM image of a working electrode used for methanol oxidation, which contained Pd NPs supported on dimpled Ni. (b) Specific current density (normalized against Pd ECSA) of methanol oxidation for a planar Pd electrode and Pd NPs loaded onto regular, dimpled features (200-nm \varnothing) in Ni. (c) An EDS spectrum of the dimpled Ni features coated with Pd nanocatalysts was prepared by focused ion beam (FIB) liftout and analyzed for their elemental content using the TEM. The Pt signal arised from the protective layer that was deposited ontop of the sample during the FIB liftout preparation.

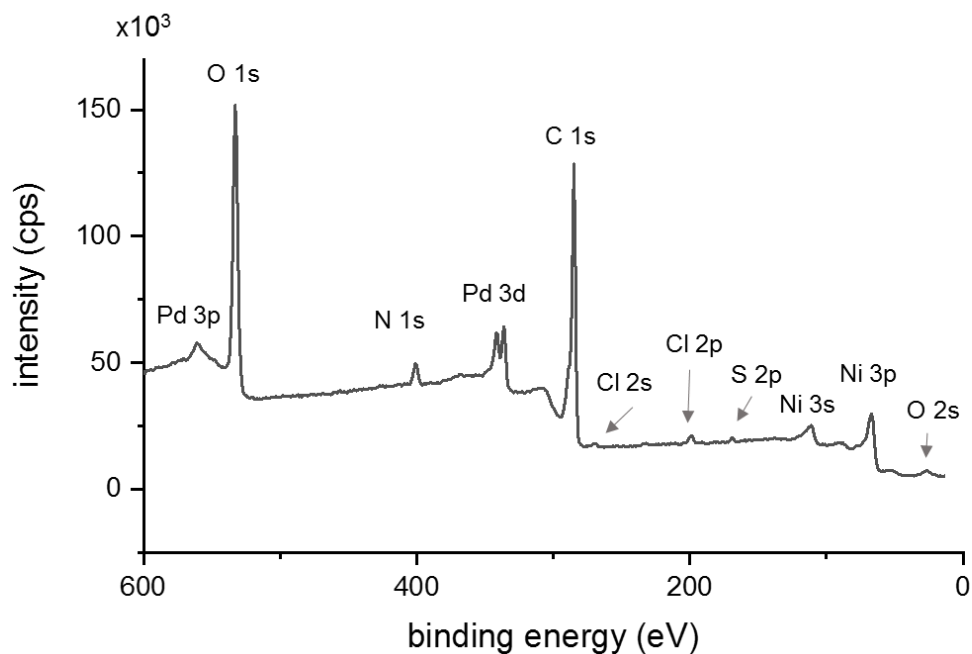


Figure S9. Results from an X-ray photoelectron spectroscopy (XPS) survey scan of Pd NPs supported on dimpled Ni following the electrochemical methanol oxidation experiments. The spectrum was obtained using a Kratos Analytical Axis Ultra DLD in 4D LABS at Simon Fraser University. The instrument was operated with a hybrid lens, an anode high tension of 15 kV, and a monochromated Al X-ray source.

References

1. M. W. Breiter, *J. Electroanal. Chem.*, 1977, **81** (2), 275-284.
2. G. F. Alvares, M. Mamlouk, and K. Scott, *Int. J. Electrochem.*, 2011, **2011**, 1-12.